

# Design Strategy for High Performance Thermoelectric Materials: the Prediction of Electron Doped KZrCuSe<sub>3</sub>

Shiqiang Hao,<sup>1</sup> Logan Ward,<sup>1</sup> Zhongzhen Luo,<sup>2</sup> Vidvuds Ozolins,<sup>3</sup> Vinayak P. Dravid,<sup>1</sup> Mercuri G. Kanatzidis,<sup>2</sup> and Christopher Wolverton<sup>1\*</sup>

<sup>1</sup>Department of Materials Science and Engineering, Northwestern University, Evanston IL 60208

<sup>2</sup>Department of Chemistry, Northwestern University, Evanston IL 60201

<sup>3</sup>Department of Applied Physics, Yale University, New Haven, Connecticut 06511, and Energy Sciences Institute, Yale University, West Haven, Connecticut 06516

## Calculation methods

### Density functional theory (DFT) calculations

The total energies and relaxed geometries were calculated by DFT within the generalized gradient approximation of Perdew-Burke-Ernzerhof for the exchange correlation functional with Projector Augmented Wave potentials.<sup>1</sup> We use periodic boundary conditions and a plane wave basis set as implemented in the Vienna *ab initio* simulation package.<sup>2</sup> The total energies were numerically converged to approximately 3meV/cation with spin-orbit coupling using a basis set energy cutoff of 500 eV and dense *k*-meshes corresponding to 4000 per reciprocal atom *k*-points in the Brillouin zone. Our theoretically relaxed KZrCuSe<sub>3</sub> lattice constants are respectively  $a=3.91\text{\AA}$ ,  $b=14.95\text{\AA}$ , and  $c=10.24\text{\AA}$ , which are in good agreement with the experimental Cmc<sub>2</sub>m crystal structure with measured lattice parameters  $a=3.87\text{\AA}$ ,  $b=14.51\text{\AA}$ , and  $c=10.16\text{\AA}$ .<sup>3</sup>

### Phonon dispersion and lattice thermal conductivity

Calculation of the lattice thermal conductivity is a very active field of research. Some work used molecular dynamics,<sup>4,5</sup> second order<sup>6</sup>, and third order force constants<sup>7</sup> methods to calculate thermal conductivity. Due to molecular dynamics and third order force constant methods are very time consuming, we apply force constant method within quasi-harmonic approximation to investigate vibrational properties.<sup>8</sup> In this method, the dynamical matrix at any  $\vec{q}$  point can be given,

---

\*Corresponding author: c-wolverton@northwestern.edu

$$D_{ij}^{\alpha\beta}(\vec{q}) = \frac{1}{\sqrt{m_i m_j}} \sum_l \Phi_{i,j}^{\alpha\beta} e^{i\vec{q}R_l} \quad (5)$$

Where  $\Phi$  is the harmonic interatomic force constant matrix,  $m$  is the atomic mass,  $R_l$  is the translation vector of the unit cell  $l$ ,  $ij$  specifies the  $i$ -th( $j$ -th) atom in the primitive cell, and  $\alpha\beta$  are Cartesian components. The eigenvalues of the dynamical matrix yield the phonon frequencies and the dispersion. In the quasi-harmonic approximation, the phonon frequencies are allowed to be volume dependent, which amounts to assuming that the force constant tensors are volume dependent.<sup>8</sup> We calculate dynamic matrix and force constant using the compressive sensing<sup>9</sup> and lattice thermal conductivity by Boltzmann transport theory<sup>10</sup> This method has recently been shown to produce very accurate values of lattice thermal conductivity, compared to experiment, for low-conductivity thermoelectric compounds.<sup>9</sup>

### Boltzmann transport calculations

To calculate the tensors of the Seebeck coefficient  $S$  and electrical conductivity  $\sigma$  we use the Boltzmann transport equation in the frame work of semiclassical transport theory.<sup>11</sup> A convenient general way of describing the collisional term in the Boltzmann equation is to define a relaxation-time  $\tau_{n,k}$  for an electron in a band  $n$  at wavevector  $k$ . Then, we obtain the following expressions for the transport tensors as a function of the electron chemical potential  $\mu$  (that depends on the doping level of the system in a semiconductor) and of the temperature  $T$ .

$$\sigma_{ij}(T, \mu) = e^2 \int -\frac{\partial f_{\mu}(T, \epsilon)}{\partial \epsilon} \sigma_{ij}(\epsilon) d\epsilon \quad (1)$$

$$(\sigma S)_{ij}(T, \mu) = \frac{e}{T} \int \left( -\frac{\partial f_{\mu}(T, \epsilon)}{\partial \epsilon} \right) (\epsilon - \mu) \sigma_{ij}(\epsilon) d\epsilon \quad (2)$$

$$\kappa_{ij}(T, \mu) = \frac{\pi^2}{3} \left( \frac{k_B}{e} \right)^2 \sigma_{ij}(T, \mu) T \quad (3)$$

Here  $\sigma S$  denotes the matrix product of the two tensors, and  $\partial f_{\mu}/\partial \epsilon$  is the derivative of the Fermi-Dirac distribution function with respect to the energy. Moreover, we have defined the above quantities in terms of the transport distribution function  $\sigma_{ij}(\epsilon)$ , defined as

$$\sigma_{ij}(\epsilon) = \frac{1}{V} \sum_{n,k} v_i(n,k) v_j(n,k) \tau_{n,k} \delta(\epsilon - \epsilon_{n,k}) d\epsilon \quad (4)$$

where the summation is over all bands  $n$  and over all the Brillouin zone,  $\epsilon_{n,k}$  is the energy for band  $n$  at  $k$  and  $v_i(n,k)$  is the  $i$ -th component of the band velocity at  $(n,k)$  as given by  $v_i(n,k) = 2\pi/\hbar \partial \epsilon_{n,k} / \partial k_i$ . Note

that the value of chemical potential depends on temperature and carrier concentration, then the transport tensors are also related to temperature and concentration. The figure of merit is defined as  $zT = \sigma S^2 T / (\kappa_{Latt} + \kappa_{elec})$ , where the power factor for different directions are respectively  $\sigma_{xx} S_{xx}^2$ ,  $\sigma_{yy} S_{yy}^2$ , and  $\sigma_{zz} S_{zz}^2$  due to linearly independent transport tensors.

## Experiment section

**Synthesis.** The raw materials used were Zr powder (99.5%, Aldrich Chemical Co., USA), Cu (99.99%, American Elements, USA), Se pieces (99.99%, American Elements, USA), K chunks (99.99%, Aldrich Chemical Co., USA).  $K_2Se$  was synthesized by a stoichiometric reaction of K and Se elements in liquid  $NH_3$  as described elsewhere.<sup>12,13</sup>  $ZrSe_2$  was synthesized by a stoichiometric reaction of Zr and Se elements in a two-zone furnace with the hot and cold zone temperature of 950 and 800 °C. The  $K_2Se$ , Cu,  $ZrSe_2$  and Se were loaded into 13 mm diameter carbon-coated quartz tube in an  $N_2$ -filled glove box. The tube was evacuated up to  $\sim 2 \times 10^{-3}$  Torr and flame-sealed, followed by reacting in programmable furnaces. The tube was slowly heated to 673 K over 8 h, then heated to 1073 K in 10 h, and soaked at this temperature for two days, then slowly cooled down to room temperature in 15 h.

**Powder X-ray Diffraction (PXRD) Characterization.** Phase purity of the synthesized sample was performed by PXRD using a Rigaku Miniflex powder X-ray diffractometer with Ni-filtered Cu  $K_\alpha$  ( $\lambda = 1.5418 \text{ \AA}$ , 40 kV and 15 mA).

**Spark Plasma Sintering (SPS).** The  $KZrCuSe_3$  fine powder was filled into a 12.7 mm diameter graphite die and densified by using the SPS technique (SPS-211LX, Fuji Electronic Industrial Co. Ltd.) at 773 K for 10 min. The applied axial compressive stress is 40 MPa. The resulting pellet had high theoretical density  $\sim 95\%$ .

**Thermal Conductivity.** The thermal diffusivity ( $D$ ) was measured by using a Netzsch Laser Flash Analysis (LFA) 457 instrument under a continuous  $N_2$  flow. The samples along two directions: parallel to the direction of applied pressure and perpendicular to the applied pressure with dimensions of  $\sim 6 \times 6 \times 1.5 \text{ mm}^3$  were cut and polished, then coated with a thin layer of graphite to prevent the emissivity of the material. The Cowan model with pulse correction was performed for data analysis. The total thermal conductivity was calculated from the relationship  $\kappa = D \cdot C_p \cdot \rho$ , where specific heat capacity  $C_p$  is obtained from the the Dulong-Petit approximation,<sup>14</sup> and the density  $\rho$  is calculated using the sample's geometry and mass.

**Band gap measurement.** The optical band gap of  $\text{KZrCuSe}_3$  was determined by a Nicolet 6700 FT-IR spectrometer with the wave number range  $4000 - 400 \text{ cm}^{-1}$ . The reflectance spectra was converted by using Kubelka-Munk equations:  $\alpha/S' = (1 - R)^2/(2R)$ , where  $\alpha$ ,  $S'$  and  $R$ , are the absorption, scattering, and reflectance coefficients, respectively.<sup>13</sup>

**Thermal transport properties.**

The thermal diffusivity ( $D$ ) with two different directions,  $\text{KZrCuSe}_3$ -Pa (parallel to the direction of applied pressure) and  $\text{KZrCuSe}_3$ -Pe (perpendicular to the applied pressure), is displayed in Figure S2. The anisotropic crystal structure of  $\text{KZrCuSe}_3$  is well supported by thermal diffusivity (Figure 1). In detail, the thermal diffusivity gradually decrease from 1.33 and  $0.7 \text{ mm}^2\text{S}^{-1}$  at 300 K to 0.62 and  $0.37 \text{ mm}^2\text{S}^{-1}$  at 673 K for  $\text{KZrCuSe}_3$ -Pe and  $\text{KZrCuSe}_3$ -Pa, respectively. The total thermal conductivity was shown in Figure S2, the same as thermal diffusivity, total thermal conductivity of  $\text{KZrCuSe}_3$ -Pa has the lower values than that of  $\text{KZrCuSe}_3$ -Pe sample. Moreover, the total thermal conductivity of  $\text{KZrCuSe}_3$ -Pa is lower than  $1 \text{ Wm}^{-1}\text{K}^{-1}$  over the entire temperature range of 300-673 K. Finally, the ultralow total thermal conductivity of  $\sim 0.5 \text{ Wm}^{-1}\text{K}^{-1}$  at 673 K was obtained for  $\text{KZrCuSe}_3$ -Pa.

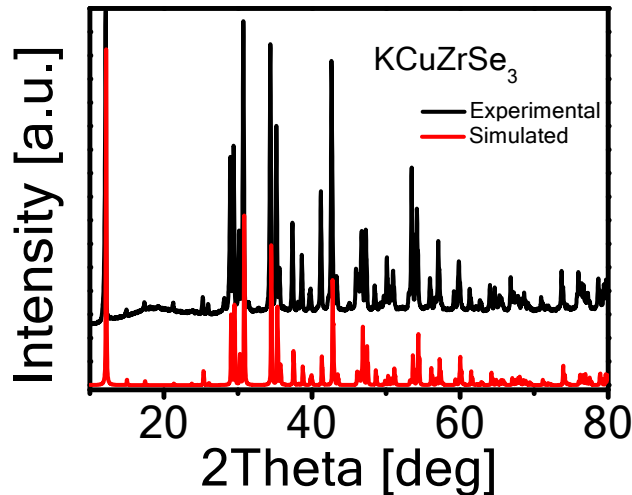


Figure S1. Experimental (black) and simulated (red) PXR patterns for  $\text{KZrCuSe}_3$

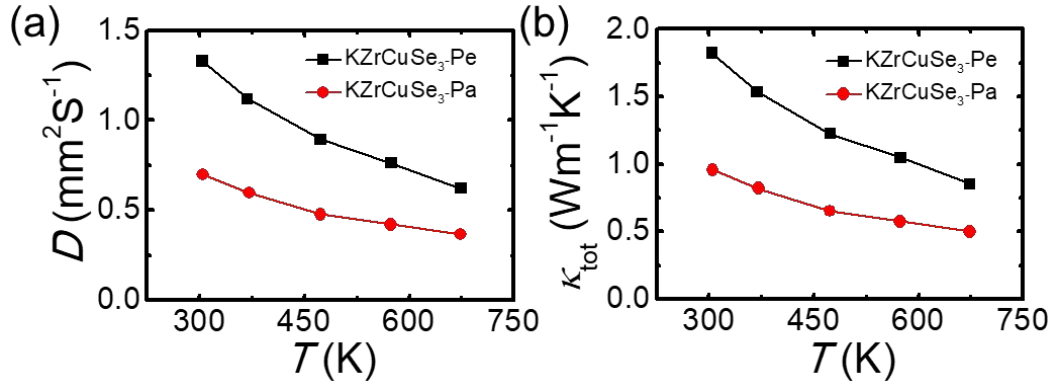


Figure S2. Temperature-dependent thermal diffusivity,  $D$  and total thermal conductivity,  $\kappa_{\text{tot}}$  for KZrCuSe<sub>3</sub>-Pe and KZrCuSe<sub>3</sub>-Pa.

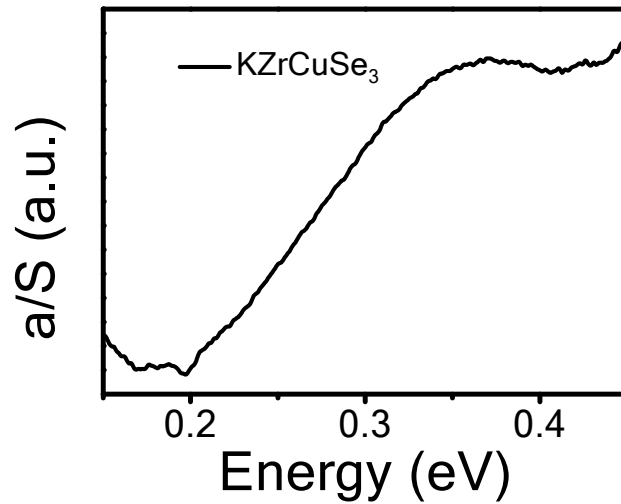


Figure S3. The electronic absorption spectra obtained from diffuse reflectance infrared spectroscopy measurement on KZrCuSe<sub>3</sub> sample.

- (1) Perdew, J. P.; Burke, K.; Ernzerhof, M. Generalized Gradient Approximation Made Simple, *Phys. Rev. Lett.* **1996**, *77*, 3865.
- (2) Kresse, G.; Furthmüller, J. Efficient iterative schemes for ab initio total-energy calculations using a plane-wave basis set, *Phys. Rev. B* **1996**, *54*, 11169.
- (3) Mansuetto, M. F.; Keane, P. M.; Ibers, J. A. Synthesis, structure, and conductivity of the new group IV chalcogenides KZrCuQ<sub>3</sub> (Q=S, Se,Te),, *J. Solid State Chemistry* **1992**, *101*, 257.
- (4) Green, M. S. Markoff Random Processes and the Statistical Mechanics of Time-Dependent Phenomena. II. Irreversible Processes in Fluids, *J. Chem. Phys.* **1954**, *22*, 398.

- (5) Kubo, R. The fluctuation-dissipation theorem, *Rep. Prog. Phys.* **1966**, *29*, 255.
- (6) Togo, A.; Oba, F.; Tanaka, I. First-principles calculations of the ferroelastic transition between rutile-type and CaCl<sub>2</sub>-type SiO<sub>2</sub> at high pressures,, *Phys. Rev. B* **2008**, *78*, 134106.
- (7) Tian, Z.; Esfarjani, K.; Chen, G. Enhancing phonon transmission across a Si/Ge interface by atomic roughness: First-principles study with the Green's function method, *Phys. Rev. B* **2012**, *86*, 235304.
- (8) Van de Walle, A.; Ceder, G. The effect of lattice vibrations on substitutional alloy thermodynamics, *Rev. Mod. Phys.* **2002**, *74*, 11.
- (9) Zhou, F.; Nielson, W.; Y. Xia; Ozolins, V. Lattice anharmonicity and thermal conductivity from compressive sensing of first-principles calculations, *Phys. Rev. Lett.* **2014**, *113*, 185501.
- (10) Li, W.; Carrete, J.; Katcho, N. A.; Mingo, N. ShengBTE: a solver of the Boltzmann transport equation for phonons, *Comp. Phys. Commun.* **2014**, *185*, 1747.
- (11) Madsen, G. K. H.; Singh, D. J. BoltzTraP. A code for calculating band-structure dependent quantities, *Comp. Phys. Commun.* **2006**, *175*, 67.
- (12) Hanco, J. A.; Sayettat, J.; Jobic, S.; Brec, R.; Kanatzidis, M. G. A<sub>2</sub>CuP<sub>3</sub>S<sub>9</sub> (A = K, Rb), Cs<sub>2</sub>Cu<sub>2</sub>P<sub>2</sub>S<sub>6</sub>, and K<sub>3</sub>CuP<sub>2</sub>S<sub>7</sub>: New Phases from the Dissolution of Copper in Molten Polythiophosphate Fluxes, *Chem. Mater.* **1998**, *10*, 3040.
- (13) McCarthy, T. J.; Ngeyi, S. P.; Liao, J. H.; DeGroot, D. C.; Hogan, T.; Kannewurf, C. R.; Kanatzidis, M. G. Molten salt synthesis and properties of three new solid-state ternary bismuth chalcogenides, .beta.-CsBiS<sub>2</sub>, .gamma.-CsBiS<sub>2</sub>, and K<sub>2</sub>Bi<sub>8</sub>Se<sub>13</sub>, *Chem. Mater.* **1993**, *5*, 331.
- (14) Zhao, J.; Islam, S. M.; Hao, S.; Tan, G.; Su, X.; Chen, H.; Lin, W.; Li, R.; Wolverton, C.; Kanatzidis, M. G. Semiconducting Pavonites CdMBi<sub>4</sub>Se<sub>8</sub> (M = Sn and Pb) and Their Thermoelectric Properties, *Chem. Mater.* **2017**, *29*, 8494.